

## Giant Negative Magnetization in a Layered Organic Magnet

Randy S. Fishman and Fernando A. Reboredo

*Materials Science and Technology Division, Oak Ridge National Laboratory, Oak Ridge, Tennessee 37831-6065, USA*  
(Received 21 May 2007; published 19 November 2007)

Bimetallic oxalates are a class of layered organic magnets with transition metals  $M(\text{II})$  and  $M'(\text{III})$  coupled by oxalate molecules in an open honeycomb structure. Energy, structure, and symmetry considerations are used to construct a reduced Hamiltonian, including exchange and spin-orbit interactions, that explains the giant negative magnetization in some of the ferrimagnetic  $\text{Fe}(\text{II})\text{Fe}(\text{III})$  compounds. We also provide new predictions for the spin-wave gap, the effects of uniaxial strain, and the optical flipping of the negative magnetization in  $\text{Fe}(\text{II})\text{Fe}(\text{III})$  bimetallic oxalates.

DOI: [10.1103/PhysRevLett.99.217203](https://doi.org/10.1103/PhysRevLett.99.217203)

PACS numbers: 75.50.Xx, 71.70.Ej, 75.10.Dg, 75.30.Gw

Compared with the burgeoning effort to synthesize and characterize organic magnets [1,2], little progress has been made in using symmetry and energy considerations to predict the magnetic behavior of organic magnets. This work closes that gap by developing the theoretical framework to design the magnetic properties of bimetallic oxalates [3], an important class of layered organic magnets. We demonstrate that, due to the spin-orbit coupling within each bimetallic layer, different choices of intercalated cations can produce large changes in the magnetic behavior.

Bimetallic oxalates are salts with the chemical formula  $A[M(\text{II})M'(\text{III})(\text{ox})_3]$ , where  $A$  is an organic cation that separates the negatively-charged metallic layers. Each of the metallic layers contains two different metal atoms in the alternating honeycomb structure pictured in Fig. 1. Neighboring metal atoms  $M(\text{II})$  with valence +2 and  $M'(\text{III})$  with valence +3 are bridged by the oxalate molecule  $\text{ox} = \text{C}_2\text{O}_4$  with valence -2. Most commonly,  $M(\text{II}) = \text{Mn}, \text{Ni}, \text{Fe}, \text{Co}, \text{Cu},$  or  $\text{Zn}$  and  $M'(\text{III}) = \text{Cr}, \text{Ru},$  or  $\text{Fe}$ . The stacking of the bimetallic planes can be rather complex with, depending on the metal and cation species, from 2 to 6 bimetallic layers per unit cell [4,5]. For different metal atoms, a single bimetallic layer can be either ferromagnetic or ferrimagnetic ( $M(\text{II})$  and  $M'(\text{III})$  moments parallel or antiparallel) with magnetic moments pointing out of the plane. While it cannot change the sign of the exchange coupling, the organic cation  $A$  does affect the overall behavior of the system. With the appropriate cation, bimetallic oxalates can be optically activated [5], metallic [6], or disordered [7,8].

The bimetallic oxalates with the highest magnetic transition temperatures are the ferrimagnetic  $\text{Fe}(\text{II})\text{Fe}(\text{III})$  compounds [9,10], where  $\text{Fe}(\text{II})$  and  $\text{Fe}(\text{III})$  have  $3d^6$  and  $3d^5$  electronic configurations, respectively. Surprisingly,  $\text{Fe}(\text{II})\text{Fe}(\text{III})$  bimetallic oxalates with certain cations exhibit giant negative magnetization (GNM) in a small field of 100 Oe: while the magnetization lies along the field direction just below the ferrimagnetic transition of about 45 K, it changes sign below about 28 K so that the mag-

netization lies opposite the magnetic field. Magnetic compensation in ferrimagnets like the rare-earth transition-metal intermetallics [11] is typically caused by the next-nearest neighbor interactions between spins on the same sublattice [12]. However, the large separation between the metal atoms on the open honeycomb structure suggests that next-neighbor interactions should be rather weak. We would like to understand why some cations produce magnetic compensation in the bimetallic oxalates while others do not.

Since the separation between the bimetallic layers for cation  $A = \text{N}(n - \text{C}_n\text{H}_{2n+1})_4$  grows from 8.2 to 10.2 Å as  $n$  increases from 3 to 5, the effect of layer separation can be systematically investigated in the  $\text{N}(n - \text{C}_n\text{H}_{2n+1})_4 \times [\text{Fe}(\text{II})\text{Fe}(\text{III})(\text{ox})_3]$  system. Unexpectedly, the transition temperature increases from 35 to 48 K with increasing layer separation (the  $n = 4$  and 5 cations are associated

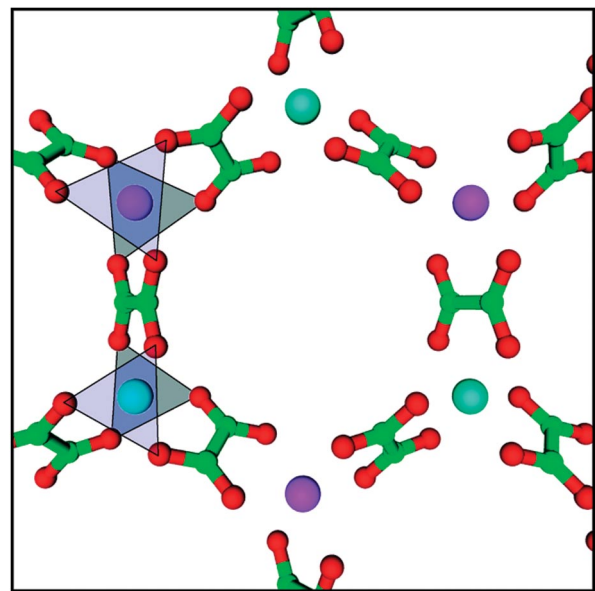


FIG. 1 (color). A portion of the bimetallic layer with  $M(\text{II})$  (blue) and  $M'(\text{III})$  (purple) coupled by oxalate  $\text{C}_2\text{O}_4$  molecules, with oxygen atoms in red and carbon atoms in green.

with GNM but the  $n = 3$  cation is not). Additional evidence comes from the observation [6,13] that a magnetic  $s = 1/2$  cation has little effect on the critical temperature and coercive field of a wide range of bimetallic oxalates. These experiments suggest that the coupling between layers is not responsible for the magnetic ordering of bimetallic oxalates. But according to the Mermin-Wagner theorem, gapless spin excitations in an isolated two-dimensional layer will destroy long-range magnetic order at nonzero temperatures. As shown below, the spin-orbit coupling within each layer explains all the available experimental data.

Like many organic magnets [12,14], the Fe(II)Fe(III) bimetallic oxalates contain three hierarchies of energies. Because of its origin in the Pauli exclusion principle on each transition metal, the Hund's coupling that fixes the spins  $S = 2$  and  $S' = 5/2$  and orbital angular momentum  $L = 2$  and  $L' = 0$  on the Fe(II) ( $3d^6$ ) and Fe(III) ( $3d^5$ ) sites is the dominant energy. Susceptibility measurements [9] confirm that both Fe(II) and Fe(III) are in their high-spin states. The  $C_3$ -symmetric crystal-field potential produced by the 6 oxygen atoms that surround each Fe atom is next in importance. Finally, the contributions to the crystal-field potential that violate  $C_3$  symmetry, the antiferromagnetic exchange coupling  $J_c \mathbf{S} \cdot \mathbf{S}'$  between the Fe(II) and Fe(III) spins, and the spin-orbit coupling  $\lambda \mathbf{L} \cdot \mathbf{S}$  on the Fe(II) site ( $\lambda < 0$  because the Fe(II) shell is more than half filled) are all considered to lie in the lowest-energy scale.

X-ray measurements [4] indicate that the oxygen atoms around each transition metal form two triangles that lie above and below the bimetallic plane. As sketched in Fig. 1, one of the triangles is a bit closer to the transition metal and a bit larger than the other triangle, which is rotated by about  $48^\circ$  from the first. The heavily-compressed,  $C_3$ -symmetric octahedral crystal field  $V(\rho, \theta, \phi)$  around each Fe(II) site can be expanded in Legendre polynomials as

$$V(\rho, \theta, \phi) = \sum_{n+3n' > 1; n, n' \geq 0} A_{n, n'} \rho^{n+3n'} P_n(\cos\theta) \times \cos(3n'\phi + \mu_{n, n'}). \quad (1)$$

The phase  $\mu_{n, n'}$  reflects the rotation of the two oxygen triangles.

After integrating over the spherical coordinates, we find that the crystal-field Hamiltonian  $H^{\text{cf}} = \langle m' | V(\rho, \theta, \phi) | m \rangle$  ( $m', m = \pm 2, \pm 1, 0$ ) can be written

$$H^{\text{cf}} = \begin{pmatrix} \gamma & 0 & 0 & \alpha & 0 \\ 0 & \gamma' & 0 & 0 & -\alpha \\ 0 & 0 & 0 & 0 & 0 \\ \alpha^* & 0 & 0 & \gamma' & 0 \\ 0 & -\alpha^* & 0 & 0 & \gamma \end{pmatrix}, \quad (2)$$

where we have subtracted off a diagonal matrix. The  $n = 2, 4$  and  $n' = 0$  terms in  $V(\rho, \theta, \phi)$  produce the diagonal  $\gamma$  and  $\gamma'$  terms, which are real; the  $n' = 1$  terms produce the off-diagonal  $\alpha$  terms, which couple the  $L = 2$  wave func-

tions with  $m - m' = \pm 3$  and may be complex due to the phases  $\mu_{n, 1}$ .

By diagonalizing  $H^{\text{cf}}$ , we obtain the low-energy orbital doublet  $|\psi_1\rangle \propto -2\alpha|2\rangle + (\gamma - \gamma' + r)|-1\rangle$  and  $|\psi_2\rangle \propto 2\alpha|1\rangle + (-\gamma + \gamma' + r)|-2\rangle$ , with degenerate energies  $\epsilon_1 = \epsilon_2 = \epsilon^{(0)} \equiv (\gamma + \gamma')/2 - r/2$  where  $r = \sqrt{(\gamma - \gamma')^2 + 4|\alpha|^2}$ . These eigenstates carry  $z$  orbital angular momentum

$$\begin{aligned} \langle \psi_1 | L_z | \psi_1 \rangle &= -\langle \psi_2 | L_z | \psi_2 \rangle \\ &= \frac{2|\alpha|^2 - (\gamma - \gamma')^2 - (\gamma - \gamma')r}{4|\alpha|^2 + (\gamma - \gamma')^2 + (\gamma - \gamma')r}. \end{aligned} \quad (3)$$

In Fig. 2,  $L_z^{\text{cf}} = |\langle \psi_1 | L_z | \psi_1 \rangle|$  depends only on the difference  $(\gamma - \gamma')/|\alpha|$  and can vary from completely quenched ( $L_z^{\text{cf}} = 0$ ) to unquenched ( $L_z^{\text{cf}} = 2$ ). The ratio  $\kappa = L_z^{\text{cf}}/2$  is commonly called the orbital reduction factor [14].

In addition to the low-energy doublet  $|\psi_{1,2}\rangle$ , a singlet  $|\psi_3\rangle = |0\rangle$  has energy  $\epsilon_3 = 0$  and an upper orbital doublet  $|\psi_{4,5}\rangle$  is obtained from  $|\psi_{1,2}\rangle$  by taking  $r \rightarrow -r$ . The solid curve in Fig. 2 denotes the condition  $\epsilon^{(0)} = 0$  or  $\gamma\gamma' = |\alpha|^2$ , where the singlet  $|\psi_3\rangle$  crosses the low-energy doublet. Since  $\langle \psi_3 | L_z | \psi_3 \rangle = 0$ , the  $z$  orbital angular momentum is completely quenched with  $L_z^{\text{cf}} = 0$  above this solid curve. If octahedral symmetry were preserved by the crystal field, then  $\epsilon^{(0)}$  would vanish and the orbital doublet  $|\psi_{1,2}\rangle$  would be degenerate with the singlet  $|\psi_3\rangle$ . With the assumption  $T \ll |\epsilon^{(0)}|$ , the singlet state is unoccupied below the solid curve and the doublet is unoccupied above.

For a magnetically anisotropic material with  $\epsilon^{(0)} < 0$  and  $L_z^{\text{cf}} > 0$ , the magnetic moments  $M = \langle 2S_z + L_z \rangle$  and

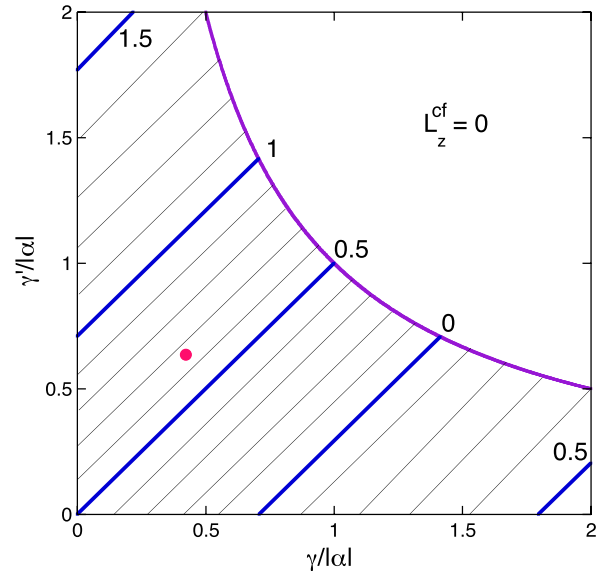


FIG. 2 (color online). A contour plot showing the effect of crystal-field parameters  $\gamma$ ,  $\gamma'$ , and  $\alpha$  on  $L_z^{\text{cf}}$ , given in increments of 0.1 by the straight lines. The orbital doublet remains lower in energy than the singlet below the solid curve, above which  $L_z^{\text{cf}} = 0$ . A rough estimate [19] based on density-functional theory gives the circular point.

$M' = \langle 2S'_z \rangle$  on the Fe(II) and Fe(III) sites (set  $\mu_B = 1$ ) are solved within mean-field theory. A reduced Hamiltonian is constructed on the Fe(II) site within the  $|\psi_1, \sigma\rangle, |\psi_2, \sigma\rangle$  subspace ( $\sigma = \pm 2, \pm 1, 0$ ) including both the exchange and spin-orbit interactions. Since all matrix elements of  $L_{\pm}$  vanish in this subspace, the spin-orbit interaction  $\lambda \mathbf{L} \cdot \mathbf{S}$  on the Fe(II) site is diagonal. So the energies of  $|\psi_1, \sigma\rangle$  and  $|\psi_2, \sigma\rangle$  are  $\epsilon_{1\sigma} = \epsilon^{(0)} + (\lambda L_z^{cf} + 3J_c M'/2)\sigma$  and  $\epsilon_{2\sigma} = \epsilon^{(0)} + (-\lambda L_z^{cf} + 3J_c M'/2)\sigma$ , where the Fe(III) moment  $M'(T) = 2S'B_{S'}(-3S'J_c \langle S_z \rangle / T) > 0$  is proportional to the spin  $S' = 5/2$  Brillouin function. It is then straightforward to evaluate the critical temperature  $T_c$  and the average magnetic moment  $M^{\text{avg}} = (M' + M)/2 = (|M'| - |M|)/2$  as a function of  $T/T_c$ . We find that  $T_c/J_c$  monotonically increases from  $\sqrt{S(S+1)S'(S'+1)} \approx 7.25$  when  $-\lambda L_z^{cf}/J_c = 0$  [15] to  $\sqrt{3S'(S'+1)S} \approx 10.25$  as  $-\lambda L_z^{cf}/J_c \rightarrow \infty$ . A similar formalism was proposed by Slonczewski for Co-doped magnetite [16].

For a strong spin-orbit coupling constant,  $\lambda = -8J_c$ ,  $M^{\text{avg}}$  is plotted versus  $T/T_c$  for various values of  $L_z^{cf}$  in Fig. 3, which takes the magnetic moment of Fe(III) to be positive. When  $0 \leq L_z^{cf} < 0.51$ , there are no compensation points and the average moment is always positive ( $|M'| > |M|$ ). In the narrow region  $0.51 \leq L_z^{cf} \leq 0.54$ , there are two compensation temperatures. For  $0.54 < L_z^{cf} < 1$ , there is a single compensation temperature above which the average moment is negative. And for  $1 < L_z^{cf} \leq 2$ , the average moment is always negative ( $|M| > |M'|$  due to the Fe(II) orbital contribution).

These results are summarized in Fig. 4, which indicates the number of compensation points  $n_{\text{comp}}$  in the  $\{-\lambda/J_c, L_z^{cf}\}$  phase space. Two regions have  $n_{\text{comp}} = 1$ : one for large spin-orbit coupling and in a range of  $L_z^{cf}$

below 1; the other for small spin-orbit coupling and  $L_z^{cf} > 1$ . In the upper-left region, the moment is negative just below  $T_c$  where the Fe(II) moment dominates and positive at low temperatures where the Fe(III) moment dominates; in the lower-right region, the moment is positive just below  $T_c$  and negative at low temperatures. The inset to Fig. 4 plots the compensation temperatures  $T_{\text{comp}}$  versus  $L_z^{cf}$  for several values of  $-\lambda/J_c$ . Since  $T_c$  increases with  $-\lambda L_z^{cf}/J_c$ , these results explain why GNM materials have higher critical temperatures [9].

The main role played by the cation in Fe(II)Fe(III) bimetallic oxalates is to slightly modify the crystal field potential by displacing the Fe(II) ions with respect to the oxalate molecules. ‘‘Normal’’ Fe(II)Fe(III) bimetallic oxalates without magnetic compensation can fall into two classes. The cations may reverse the distortion of the octahedral crystal field so that  $\epsilon^{(0)} > 0$  with the  $L_z^{cf} = 0$  singlet lying lower in energy than the orbital doublet. Since there is no magnetic anisotropy when  $L_z^{cf} = 0$ , GNM would be absent as well. Alternatively, the orbital doublet may remain lower in energy but with a small  $L_z^{cf} > 0$  falling into the left  $n_{\text{comp}} = 0$  region of Fig. 4.

Our results for  $T_{\text{comp}}$  and  $T_c$  can be used to estimate the experimental parameters for bimetallic oxalates that exhibit GNM. Taking the value of  $\lambda \approx -10^2 \text{ cm}^{-1}$  or  $-12.65 \text{ meV}$  from paramagnetic resonance measurements of Fe(II) [17] and the estimate  $T_{\text{comp}}/T_c = 0.62$  from experiments on GNM materials [9] gives  $J_c \approx 0.46 \text{ meV}$  and  $L_z^{cf} \approx 0.28$  [18]. For  $\lambda/J_c = -27.5$ ,  $n_{\text{comp}} = 0$  when  $L_z^{cf} < 0.23$  so that GNM materials lie just inside the

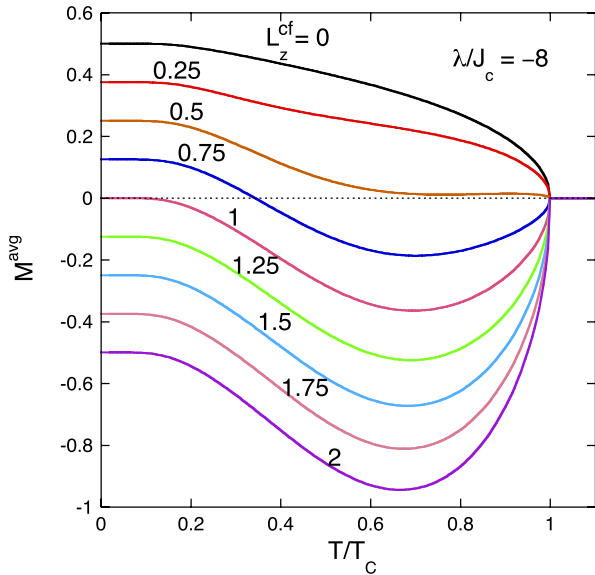


FIG. 3 (color online). The average magnetic moment versus  $T/T_c$  for various  $L_z^{cf}$  and  $\lambda/J_c = -8$ . The Fe(III) moment is defined to be positive.

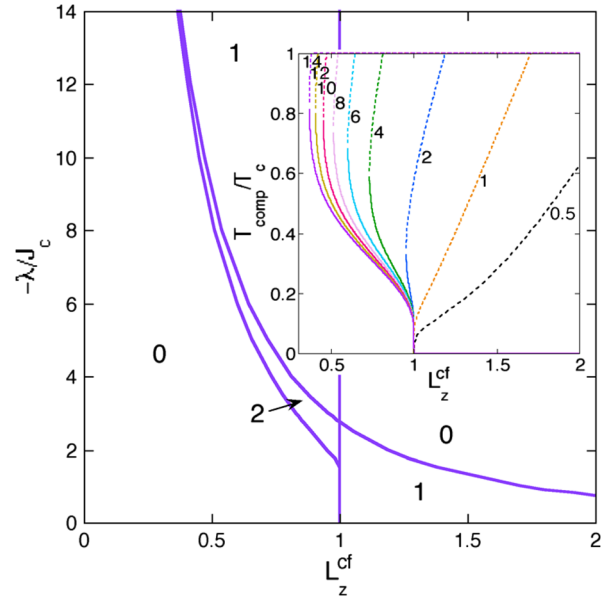


FIG. 4 (color online). A phase diagram of the magnetic behavior denoting the number of compensation points  $n_{\text{comp}} = 0, 1, \text{ or } 2$  for  $-\lambda/J_c$  versus  $L_z^{cf}$ . GNM occurs in regions with  $n_{\text{comp}} = 1$ . Inset is a plot of  $T_{\text{comp}}/T_c$  versus  $L_z^{cf}$  for various values of  $-\lambda/J_c$ .

upper-left region of Fig. 4 with  $n_{\text{comp}} = 1$  [19]. Mössbauer spectroscopy [9] confirms that the Fe(II) moment in GNM compounds dominates just below  $T_c$ , as anticipated for this region of Fig. 4. Additional support for Fig. 4 comes from the recent discovery [20] of an Fe(II)Fe(III) bimetallic oxalate with  $n_{\text{comp}} = 2$ .

The persistence of negative magnetization is associated both with the finite energy barrier  $-2\lambda L_z^{\text{cf}} S$  for flipping  $\langle L_z \rangle$  once it is aligned parallel to the magnetic field and with the small matrix element for this dipole-allowed transition (due to the hybridization of the  $L = 2$  and  $L = 1$  wave functions by the nonspherical crystal-field potential  $V(\rho, \theta, \phi)$ ). By optically exciting the higher-energy state of the orbital doublet with far-infrared light of frequency  $-2\lambda L_z^{\text{cf}} S \approx 14$  meV or wavelength  $88.5 \mu\text{m}$ , it should be possible to flip the magnetic moment in a negative-magnetization state below  $T_{\text{comp}}$ . Optical control of the magnetization has been previously demonstrated in a Mn(II)Cr(III) bimetallic oxalate [5] and other organic magnets [21].

Because it is associated with the non- $C_3$  symmetric crystal-field potential  $V_s \propto \sin\theta \cos 2\phi$ , uniaxial strain in the plane of the bimetallic layers will mix  $|\psi_1\rangle$  and  $|\psi_2\rangle$  and lower the orbital angular momentum of the ground-state orbital doublet. Consequently, uniaxial strain will decrease  $T_c$  and increase  $T_{\text{comp}}$ , eventually transforming a GNM material into a normal one.

Finally, we have performed a Holstein-Primakoff expansion to evaluate the spin-wave (SW) frequencies of Fe(II)Fe(III) bimetallic oxalates. In zero field, the SW gap is given by

$$\Delta_{\text{sw}} = \lambda L_z^{\text{cf}}/2 - 3J_c(S' - S)/2 + \{9J_c^2(S' - S)^2 + (\lambda L_z^{\text{cf}})^2 - 6\lambda L_z^{\text{cf}} J_c(S' + S)\}^{1/2}/2, \quad (4)$$

which vanishes like  $-\lambda L_z^{\text{cf}} S/(S' - S)$  as  $-\lambda L_z^{\text{cf}} \rightarrow 0$  and approaches  $3J_c S$  as  $-\lambda L_z^{\text{cf}}/J_c \rightarrow \infty$ . Using the parameters estimated above, we obtain  $\Delta_{\text{sw}} \approx 1.65$  meV, which should be relatively simple to observe with inelastic neutron-scattering techniques. The SW gap explains the high transition temperatures of well-separated two-dimensional layers, where gapless spin excitations would suppress the critical temperature.

To conclude, we have derived from structure, symmetry, and energy considerations a reduced Hamiltonian that explains all of the important observations about an important class of layered organic magnets. We have made new predictions, with potential technological implications, for the optical and mechanical control of the negative-magnetization state.

We gratefully acknowledge useful conversations with Juana Moreno. This research was sponsored by the Laboratory Directed Research and Development Program of Oak Ridge National Laboratory, managed by UT-

Battelle, LLC for the U. S. Department of Energy under Contract No. DE-AC05-00OR22725 and by the Division of Materials Science and Engineering of the U. S. DOE.

- 
- [1] J. S. Miller and A. J. Epstein, MRS Bull. **25**, 21 (2000); J. S. Miller, Adv. Mater. **14**, 1105 (2002).
  - [2] S. J. Blundell and F. L. Pratt, J. Phys. Condens. Matter **16**, R771 (2004).
  - [3] H. Tamaki *et al.*, J. Am. Chem. Soc. **114**, 6974 (1992).
  - [4] R. Pellaux *et al.*, Inorg. Chem. **36**, 2301 (1997).
  - [5] S. Bénard *et al.*, J. Am. Chem. Soc. **122**, 9444 (2000); S. Bénard, E. Rivière, P. Yu, K. Nakatani, and J. F. Delouis, Chem. Mater. **13**, 159 (2001).
  - [6] E. Coronado, J. R. Galán-Mascarós, C. J. Gómez-García, and V. Laukhin, Nature (London) **408**, 447 (2000).
  - [7] A. Alberola, E. Coronado, J. R. Galán-Mascarós, C. Giménez-Saiz, and C. J. Gómez-García, J. Am. Chem. Soc. **125**, 10774 (2003).
  - [8] I. D. Watts, S. G. Carling, P. Day, and D. Visser, J. Phys. Chem. Solids **66**, 932 (2005).
  - [9] C. Mathonière, C. J. Nuttall, S. G. Carling, and P. Day, Inorg. Chem. **35**, 1201 (1996).
  - [10] M. Clemente-León, E. Coronado, C. J. Gómez-García, and A. Soriano-Portillo, Inorg. Chem. **45**, 5653 (2006).
  - [11] J. Ostoréro and M. Guillot, J. Appl. Phys. **99**, 08M305 (2006).
  - [12] J. B. Goodenough, *Magnetism and the Chemical Bond* (Interscience, New York, 1963).
  - [13] M. Clemente-León, E. Coronado, J. R. Galán-Mascarós, and C. J. Gómez-García, Chem. Commun. (Cambridge) (1997) 1727.
  - [14] O. Kahn, *Molecular Magnetism* (VCH, New York, 1994).
  - [15] Because of two-dimensional fluctuations not included in mean-field theory,  $T_c$  should vanish as  $-\lambda L_z^{\text{cf}}/J_c \rightarrow 0$ . But when  $-\lambda L_z^{\text{cf}}/J_c \gg 1$ , the presence of a spin-wave gap  $\Delta_{\text{sw}}$  implies that the mean-field prediction for  $T_c$  should be fairly accurate.
  - [16] J. C. Slonczewski, Phys. Rev. **110**, 1341 (1958).
  - [17] B. Bleaney and K. W. H. Stevens, Rep. Prog. Phys. **16**, 108 (1953).
  - [18] A comparison of the predicted  $M^{\text{avg}}$  with the experimental measurements [9] suggests that about 15% of the domains in the low-temperature negative-magnetization state have flipped to align with the 100 Oe external field.
  - [19] A rough calculation of the crystal-field potential based on the oxygen positions for a Mn(II)Cr(III) system [4], assuming that each of the oxygens has the same charge, and integrating over the  $d$  orbitals of Fe(II) evaluated from density-functional theory yields  $\gamma/|\alpha| = 0.42$ ,  $\gamma'/|\alpha| = 0.64$ , and  $L_z^{\text{cf}} = 0.66$ , as indicated in Fig. 2.
  - [20] G. Tang, Y. He, F. Liang, S. Li, and Y. Huang, Physica (Amsterdam) **392B**, 337 (2007).
  - [21] See, D. A. Pejaković, C. Kitamura, J. S. Miller, and A. J. Epstein, Phys. Rev. Lett. **88**, 057202 (2002), and other papers referenced therein.